Photochemistry of the Indoor Air Pollutant Acetone on Degussa P25 TiO_2 Studied by Chemical Ionization Mass Spectrometry

Catherine M. Schmidt, Avram M. Buchbinder, Eric Weitz, and Franz M. Geiger*

Department of Chemistry and the Institute for Catalysis and Energy Processes, Northwestern University, 2145 Sheridan Road, Evanston, Illinois 60208

Received: August 22, 2007; In Final Form: October 1, 2007

We have used chemical ionization mass spectrometry (CIMS) to study the adsorption and photochemistry of several oxygenated organic species adsorbed to Degussa P25 TiO_2, an inexpensive catalyst that can be used to mineralize volatile organic compounds. The molecules examined in this work include the common indoor air pollutant acetone and several of its homologs and possible oxidation and condensation products that may be formed during the adsorption and/or photocatalytic degradation of acetone on titanium dioxide catalysts. We report nonreactive uptake coefficients for acetone, formic acid, acetic acid, mesityl oxide, and diacetone alcohol, and results from photochemical studies that quantify, on a per-molecule basis, the room-temperature photocatalytic conversion of the species under investigation to CO_2 and related oxidation products. The data presented here imply that catalytic surfaces that enhance formate and acetate production from acetone precursors will facilitate the photocatalytic remediation of acetone in indoor environments, even at room temperature.

I. Introduction

Indoor air pollution presents an increasing domestic environmental concern[1] because people in developed countries spend the majority of their time indoors,[2] and indoor air is often more polluted than outdoor air.[3−5] Although increased air ventilation rates can reduce indoor air pollution,[6] this remediation strategy generally increases utility and energy expenses.[7−9] Novel indoor air pollution remediation technologies that avoid a concomitant increase in the energy burden for indoor environments have therefore become highly attractive.[10−12] Heterogeneous photocatalysis is a promising strategy for remediating indoor air pollutants and has received considerable attention as a means of degrading volatile organic compounds (VOCs)[12−21] found indoors.

In environmental science, much emphasis has been placed on photocatalytic remediation using the inexpensive photocatalyst titanium dioxide.[15,17,19,22−25] In photochemical processes involving semiconductors such as TiO_2, the absorption of light creates electron-hole (e−h) pairs[15,17,26] whose excess free energy provides the driving force for subsequent photocatalytic reactions[27] that can be exploited to degrade pollutant species in enclosed indoor spaces. These indoor pollutants include oxygenated organic compounds such as aldehydes, ketones, and alcohols present at low concentrations.[28,29] Laboratory studies modeling VOC degradation over TiO_2 catalysts have frequently focused on acetone as a model pollutant because it is found in appreciable concentrations in indoor air streams.[4,30−35] Acetone also represents a highly relevant model system for other ketones found in indoor air.[1,30,31,36,37]

Proposed mechanisms for the oxidation of acetone over TiO_2-based catalysts found in the literature include several possible reaction routes. In general, the thermal[38] and photooxidation[24,25,29,39−45] of acetone have both been reported to produce CO_2 and water. Intermediates observed or postulated for this reaction include acetic acid,[38,46] formic acid,[38,43] and acetaldehyde.[43] Several literature studies also propose the formation of higher molecular weight carbon-containing species from acetone,[47] including mesityl oxide[24,48−50] and diacetone alcohol,[48,49] and hexane and hexadiene arising from secondary reactions of such aldol products.[51] The photochemistry of acetone on TiO_2 may involve radical species,[17,52,53] including peroxy radicals ($CH_3CO-CH_2OO^{\bullet}$) observed via EPR[52] and methyl radicals observed during TPD and photodesorption studies of low-temperature (95 K) photooxidation reactions of acetone on TiO_2 (110).[53] Clearly, multiple species are observed during acetone degradation, some of which are the desired mineralization products, some of which are sinks, and some of which may be catalytic poisons.[51,54]

In the extensive work regarding the interaction of acetone with TiO_2-based catalysts, fundamental studies performed at reactant partial pressures that are representative of indoor environments remain sparse. Here, we fill this void by applying chemical ionization mass spectrometry (CIMS) to study the adsorption and photochemistry of several oxygenated organic species adsorbed to Degussa P25 TiO_2 under reactant partial pressures commonly found indoors. Working at environmentally representative partial pressure conditions is crucial when considering the nonlinear relationship between gas phase concentration and surface coverage, which is not known *a priori*,[55,56] but which must be determined experimentally for those partial pressures that are representative of indoor environments. In an effort to better understand the role and surface activity of the species implicated in acetone oxidation mechanisms at the VOC partial pressures and temperatures that are present in indoor environments, and on powdered catalyst samples rather than single-crystal TiO_2, CIMS experiments were performed for several individual species (Table 1). We examined the adsorption and photooxidation of acetone, as well as that of mesityl oxide and diacetone alcohol. It has been reported that acetone coupling reactions on catalytic surfaces can result in surface equilibria between acetone, the acetone aldol product diacetone alcohol,[48,49,57,58] and the dehydrated aldol condensation product mesityl oxide.[24,39,48,50,54,58−62] Acetate and formate have

* To whom correspondence should be addressed. E-mail: f-geiger@northwestern.edu.

10.1021/jp076745+ CCC: $37.00
Published on Web 11/22/2007

TABLE 1: Analytes Studied in This Work[a]

Molecule	Formula	Structure	Protonated Parent Ion [m/z]	Proton Affinity [kJ mol^{-1}]	CIMS Spectra
Acetone	C_3H_6O		59	812	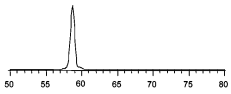
Formic Acid	CH_2O_2		47	742.0	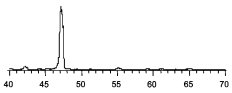
Acetic Acid	$C_2H_4O_2$		61	783.7	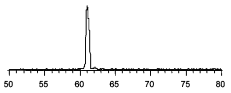
Mesityl Oxide	$C_6H_{10}O$	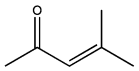	99	878.7	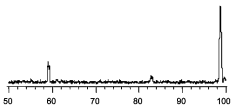
Diacetone Alcohol	$C_6H_{12}O_2$	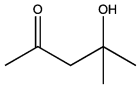	117	822.9	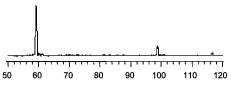
Carbon dioxide	CO_2		45	540.5	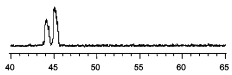
Water (CI reagent)	H_2O		19	691	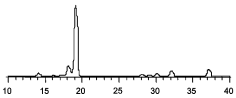

[a] Proton affinities are taken from ref 74.

also been proposed as possible reaction intermediates in acetone photocatalytic and thermal oxidation processes.[24,38,43,49,50,53,63,64] We therefore included acetic acid and formic acid, in addition to acetone, mesityl oxide, and diacetone alcohol, in our list of analytes that may be important in indoor acetone remediation, and determined their binding properties and photochemical reactions.

In this work, we first determined the individual uptake coefficients for acetone, formic acid, acetic acid, mesityl oxide, and diacetone alcohol interacting with powdered TiO_2 samples at room temperature and under environmentally representative partial pressures. To our knowledge, most of these values are not currently reported for partial pressures that are environmentally representative. After allowing these species to interact with thin Degussa P25 TiO_2 catalyst coatings, UV illumination was used to initiate photodegradation and reaction products were tracked using CIMS. These experiments yield the relative photodegradation efficiencies for the VOCs on Degussa P25 for conditions representative of indoor environments. A better understanding of the relative binding efficiencies and photooxidation potentials of the possible intermediates that are relevant to the photocatalytic oxidation of acetone is a necessary prerequisite for the rational design of catalysts that can improve indoor air quality.

II. Experimental Conditions

1. CIMS System and Catalyst Preparation. The experimental system has been described in detail elsewhere,[65] but a number of modifications were made to allow photocatalytic work in the UV regime. Briefly, a quadrupole mass spectrometer (QMS) is coupled to a quartz flow tube (~1 Torr total pressure), which holds a catalyst coated quartz insert and a movable analyte injector. Water is used as the chemical ionization reagent. The CIMS system monitors the gas phase with chemical specificity and is sensitive to environmentally relevant VOC partial pressures as low as 10^{-8} Torr.[65,66] Catalyst coatings for this work were prepared by the method described in detail previously.[65] In this procedure, we coat cylindrical quartz flow tube inserts with Degussa P25 TiO_2 (~1 mg of TiO_2/cm of catalyst length). Scanning electron microscope images (not shown) of representative samples of Degussa P25 on quartz slides indicate thicknesses for 5 and 10 layers of TiO_2 on quartz microscope slides (ChemGlass, 25 mm × 25 mm × 1 mm) of ~500 and 1000 nm, respectively.

2. Chemicals Used. Millipore water vapor provided the chemical reagent in all CIMS experiments. Commercially available helium (AirGas, Ultra High Purity) was used as both the carrier and diluting gas. Analyte samples were prepared by expanding vapor from a liquid sample into a gas transfer manifold (base pressure of 15−30 mTorr) and diluting with helium. Analytes used in this work include acetone (BDH, 99.9%), formic acid (Acros Organics, 99%), glacial acetic acid (Mallinckrodt, 80% acid by mass), mesityl oxide (Aldrich, 90%), and diacetone alcohol (Acros Organics, 99%+ GC grade). All organic compounds were used following a brief low-pressure (<50 mTorr) pump-down cycle to remove any highly volatile impurities. Mesityl oxide and diacetone alcohol samples were additionally characterized using NMR and FTIR spectroscopies (*vide infra*). Catalyst samples were prepared using titanium dioxide (Degussa P25, ~80% anatase, ~20% rutile).

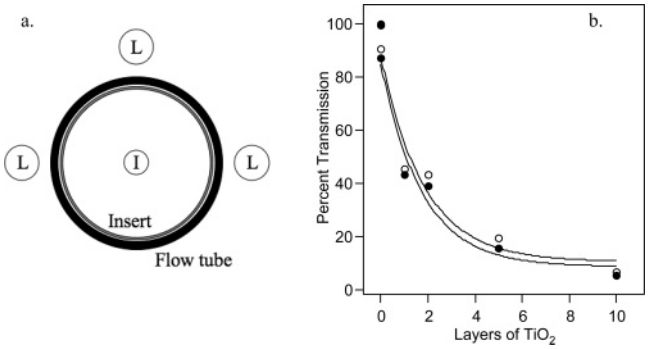

Figure 1. (a) Cartoon of a cross-section of the CIMS flow tube and UV light sources, with movable injector marked "I" and UV lights marked with "L". (b) Transmission of light as a function of TiO_2 catalyst coating thickness at the wavelengths produced by PenRay Hg lamps. Filled circles are transmission at 254 nm, and open circles are transmission at 365 nm. Exponential fits to the transmission data, which follow the form $y = Ae^{-Bl} + C$, where l is the number of TiO_2 layers, are shown, and fitting parameters are presented in Table S1 of the Supporting Information.

3. Analyte Characterization. CIMS spectra of diacetone alcohol and mesityl oxide exhibit peaks at molecular weights corresponding to species other than the protonated parent ion, which is normally the dominant signal (Table 1).[67] For mesityl oxide, CIMS spectra display a peak at the position expected for acetone and an apparent fragment at ~82 amu. For diacetone alcohol, peaks are visible at the positions expected for acetone and mesityl oxide, and the parent ion signal is only clearly visible in the spectrum at partial pressures greater than 2×10^{-5} Torr. Chemical analysis of the samples via NMR spectroscopy and gas phase FTIR spectroscopy (see Supporting Information for details) show that the mass peaks in mesityl oxide and diacetone alcohol CIMS spectra result from fragmentation in the CIMS rather than from sample contamination.

4. Photochemistry. Photochemistry is initiated by illuminating the surface with three low-intensity mercury Pen-Ray lamps (UVP, Upland, CA; 9 cm lighted length, ~4 mW/cm^{-2}) that produce principal emission lines at 254 and 365 nm. The lamps are mounted evenly around the exterior of the flow tube assembly (Figure 1a).[65,66] UV−vis spectroscopy of the catalyst coatings verify that the coatings are not opaque to UV light (Figure 1b, and Supporting Information for details). Even for the thickest coatings examined, the entire catalyst coating is exposed to light, transmitting ~6% of the incident radiation. The UV light sources we employ raise the air temperature surrounding the CIMS flow tube by 5−6 degrees to approximately 300 K. Any oxidation observed at this temperature is expected to be the result of a photochemical rather than a thermal pathway.[38]

To monitor the interaction and photoreactivity of the analytes under investigation with the catalyst coating, their CIMS signals are recorded as a function of time while exposing 5 cm of the catalyst coating formed from 10 layers of Degussa P25 on the quartz insert. For these experiments, the flow injector, without the analyte flowing, is initially positioned to expose 5 cm of catalyst film. To prevent unintentional catalyst activation, the room and UV lights are turned off, and a background CIMS signal is collected at each mass of interest. Next, the analyte is introduced into the flow tube at a given partial pressure, which is controlled using a mass flow controller (MKS). In the resulting CIMS versus time traces, the analyte CIMS signal slowly increases as the catalyst coating becomes saturated by the analyte molecules adsorbing from the gas phase (*vide infra*, Section III.1). Saturation in this case does not necessarily imply all available surface sites are filled, i.e., that monolayer coverage is achieved. Rather, the system reaches steady state at the given analyte partial pressure. After a ~170 min exposure, the analyte flow is rapidly reduced to zero. At this point, the three UV lamps surrounding the flow tube are simultaneously turned on to initiate photochemistry. Gas phase species, including photochemical reaction products, are monitored by tracking the CIMS versus time traces for all species detected.

III. Results and Discussion

1. Surface Binding Analyses. One factor controlling the efficiency of heterogeneous chemistry is the reactant surface coverage, which is dependent on the propensity of a molecule to adsorb onto the surface. Therefore, we determined the uptake coefficient, i.e., the ratio of adsorbed molecules to the surface collision flux, for each analyte. For each experiment, the resulting CIMS versus time traces (Figure 2a), which are used to determine the number of molecules lost from the gas phase to the catalyst, appear sigmoidal, with a time delay between the initial (no analyte present) and final (analyte present) equilibrium signal levels. In previous work, we showed that the sigmoidal signal shape in the presence of the catalyst coating results from an analyte−TiO_2 interaction and not the flow profile in the flow tube.[65] In these traces, the integrated area between the initiation of analyte flow ($x = 0$ in Figure 2) and the attainment of an equilibrium value ($y = 0$ in Figure 2) is representative of the number of molecules lost from the gas phase to the catalyst coating. The area in counts is multiplied by the instrument sensitivity for each analyte in molecules cm^{-3}/count, and by the length of catalyst exposed to calculate the number of molecules adsorbed onto the catalyst surface from the gas phase in molecules cm^{-2}. To calculate the number of molecules striking the surface during the saturation process, we employ the standard wall collision flux, Z_w.[68] For each analyte partial pressure, the number of molecules colliding with the catalyst coating per unit time and unit area, Z_w, is multiplied by the time interval between the initiation of analyte flow and the attainment of steady state, i.e., the same time over which the area was found above. Dividing the surface coverage obtained from the dynamic CIMS experiments by the collision flux yields the overall uptake coefficient for each analyte at each partial pressure studied (Figure 2b, and Table SI.2 in the Supporting Information). We note that the uptake coefficient determination for diacetone alcohol represents a challenge because the CIMS signal for the parent ion is negligible at the partial pressures of interest. As such, two values are reported: the uptake coefficient calculated on the basis of the signal intensity at 59 amu and the uptake coefficient calculated on the basis of the signal intensity at 99 amu.

Our uptake coefficients are in good agreement with those reported for other carbonyl compounds on TiO_2, 9.4×10^{-5} for acetaldehyde, to 3.6×10^{-4} for acetone, and 1.5×10^{-4} for propionaldehyde,[47] as well as with our own prior measurements for acetone on Degussa P25.[65] Each of the species studied exhibits a qualitatively similar propensity to bind to the catalyst surface. Diacetone alcohol binds more efficiently than the other species, probably due to the additional hydrogen-bonding capability of the alcohol.

On the basis of the data in Figure 2B, acetic and formic acids have somewhat lower uptake coefficients than the other analytes. These acids are expected to dissociate on the TiO_2 surface to form carboxylate species:[69−72] this dissociation process is activated.[73] The lower calculated uptake coefficients may be a reflection of an activation energy for dissociative adsorption.

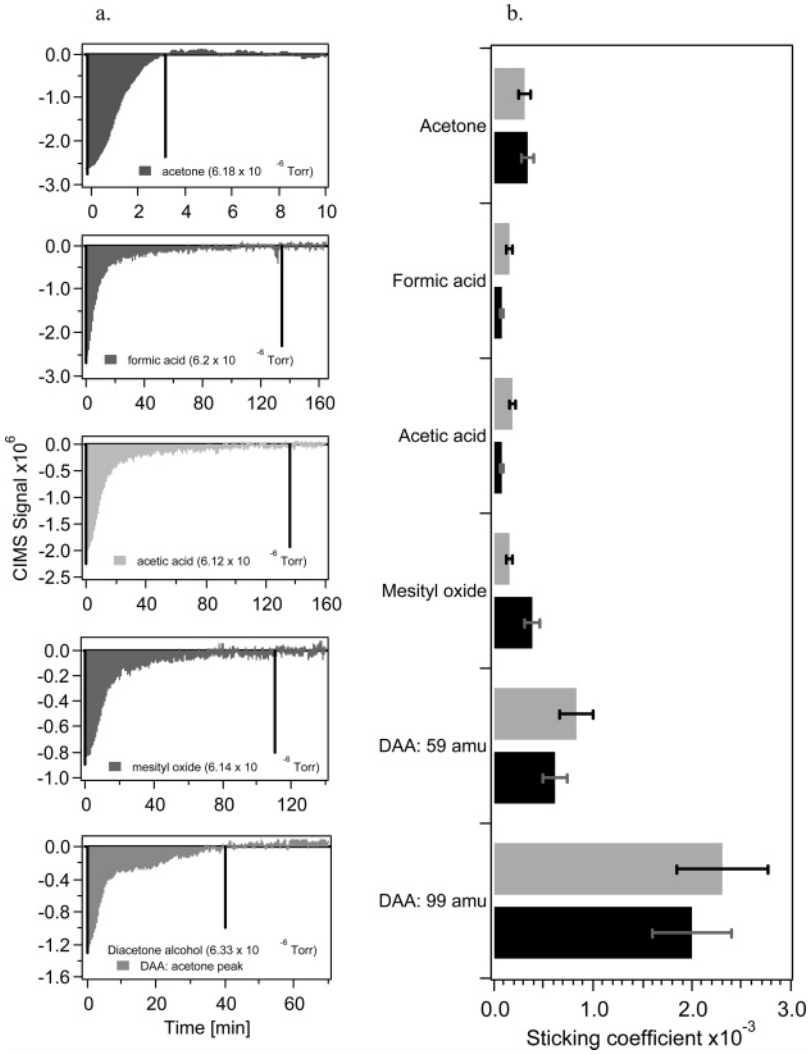

Figure 2. (a) Representative CIMS versus time traces for carbonyl uptake onto Degussa P25 catalyst coatings. For diacetone alcohol, the CIMS signal at 59 amu versus time trace is shown; the trace for 99 amu is analogous. Solid black lines indicate the time at which the catalyst reaches saturation. Note different *x*- and *y*-axes for different analytes. (b) Average uptake coefficients for these analytes for exposures of 1×10^{-6} Torr (gray bars) and 6×10^{-6} Torr (black bars). For diacetone alcohol, two values are reported: the value "DAA: 59 amu" represents the uptake coefficient as measured using the CIMS signal at 59 amu, and the value "DAA: 99 amu" represents the uptake coefficient as measured using the CIMS signal at 99 amu.

The similar values for the other analytes, particularly acetone and mesityl oxide, may imply similar binding mechanisms for each species, most likely involving hydrogen bonding through the carbonyl group. We note that the uptake coefficients reported here are for environmentally representative partial pressures of the VOCs studied.

To verify whether the interaction of acetic and formic acid with TiO_2 is indeed stronger than that of the molecularly adsorbed species, which would be expected if the acids chemisorb on the surface, a competition experiment was performed. For this experiment, a second injector was added to the experimental system parallel to the first. Using this dual-injector system, 10 cm of catalyst coating was exposed to 4.6×10^{-7} Torr acetone. As with the uptake coefficient measurements described above, the CIMS versus time trace for acetone displays a sigmoidal shape, taking greater than 30 min to reach steady state (Figure 3, lower panel, light gray trace). In contrast, the instrument response for acetone with no TiO_2 exposure, i.e., the time it takes the CIMS signal to reflect a change in acetone partial pressure in the flow tube, is near 1 min (Figure 3, upper panel). Next, we carried out the same experiment with 2×10^{-6} Torr acetic acid, which was first adsorbed onto a new catalyst coating and then allowed to desorb by moving the acetic acid injector to the front of the flow tube beyond the catalyst coating. When the acetic acid CIMS signal was stable, the same 10 cm of catalyst coating was exposed to 4.6×10^{-7} Torr acetone. In contrast to the acetone exposure without acetic acid pre-exposure, the CIMS versus time trace in this case resembles a step function, reaching steady state in only 100 s (Figure 3, lower panel, dark gray trace). The dramatic difference between this saturation time and that in the system without acetic acid pre-exposure indicates that acetone adsorption is greatly inhibited by the presence of acetic acid on the surface, implying that acetic acid does not fully desorb and that the resulting surface species are not easily displaced by physisorbing acetone molecules. This finding is consistent with a situation where dissociative adsorption of the two carboxylic acids on these powdered catalyst surfaces produces carboxylate species, while the other analytes are likely physisorbed on the surface.

2. Heterogeneous Photochemistry. A second aim of this work was to determine whether the CIMS could detect gas-phase organic intermediates discussed in the introduction that are relevant to indoor air pollution remediation conditions. Since acetone condensation products may act as catalytic poisons,[51,54] the binding and reactivity of these species at partial pressures representative of indoor environments are of particular

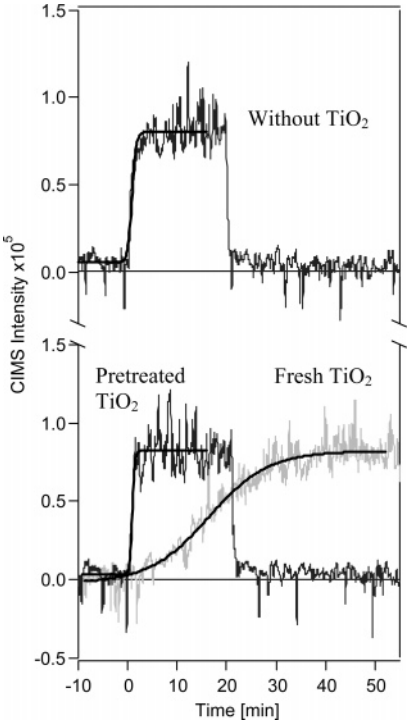

Figure 3. Acetone CIMS signal versus time traces for acetone adsorption (4.6×10^{-7} Torr acetone) with and without acetic acid surface pretreatment. Upper panel: Instrument response with no TiO_2 catalyst present. Lower panel: the light gray trace is acetone adsorption onto untreated titanium dioxide, and the dark gray trace is acetone adsorption onto TiO_2 pretreated by adsorbing 2×10^{-6} Torr acetic acid prior to acetone adsorption.

interest. The photochemistry experiment described in section II4 is therefore performed individually for acetone, formic acid, acetic acid, mesityl oxide, and diacetone alcohol, each in duplicate at partial pressures of approximately 1×10^{-6} and 6×10^{-6} Torr, while probing the gas phase for photocatalytic oxidation products. Few gas phase organic intermediates are observed in the photoreactions under these conditions, and therefore the CIMS signal corresponding to CO_2 was used to monitor the relative oxidation efficiency of these species.

a. Photooxidation of Acetone, Formic Acid, and Acetic Acid. To begin our photochemical work, we measure the gas phase photodegradation of 1.2×10^{-6} Torr acetone continuously flowing through the system without Degussa P25. In this control experiment, a slight increase is seen in the CIMS spectrum at mass to charge ratio of ~45 (recorded between 44.6 and 45.8, Figure 4), which is assigned to the acetone oxidation product CO_2 (see Supporting Information). Following this control experiment, duplicate trials of acetone photodegradation following adsorption onto TiO_2 catalyst coatings were examined. The CIMS signal versus time traces for the CO_2 signal at 45 amu are also shown in Figure 4. Following a ~3 h exposure, only a small CO_2 signal increase is observed when the UV lights are turned on, indicating that if catalyzed mineralization is occurring, the extent of oxidation is near the detection limit of the CIMS system. Based on the low acetone partial pressures used in this work, which are expected to result in low acetone surface coverages ($(1-2) \times 10^{12}$ molecules cm^{-2}),[65] this is not surprising. In addition, the small amount of observable carbon dioxide may be due to the fact that the proton affinity, which is a key parameter is CIMS studies using H_3O^+ as the reagent ion, is low for CO_2 as compared to organic carbonyl species (Table 1).[74,75]

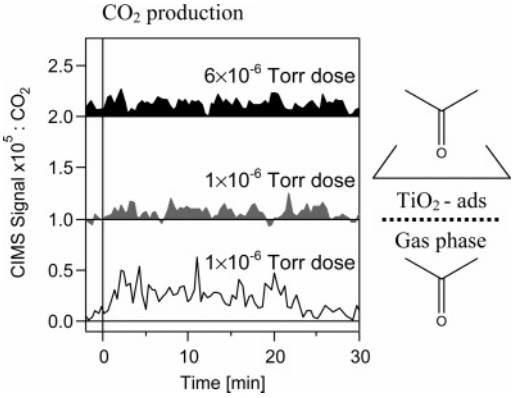

Figure 4. CO_2 production from acetone samples. The bottom trace is gas phase photolysis of $\sim 1 \times 10^{-6}$ Torr acetone. Light gray and black traces follow acetone adsorption onto 10 layers TiO_2 at $\sim 1 \times 10^{-6}$ and $\sim 6 \times 10^{-6}$ Torr acetone, respectively. Traces have been offset vertically for clarity. In all cases, UV lights were turned on at 0 min. In the gas phase trace (bottom, unfilled), UV lights were turned off at ~25 min, whereas for others UV lights remain on throughout the time interval displayed.

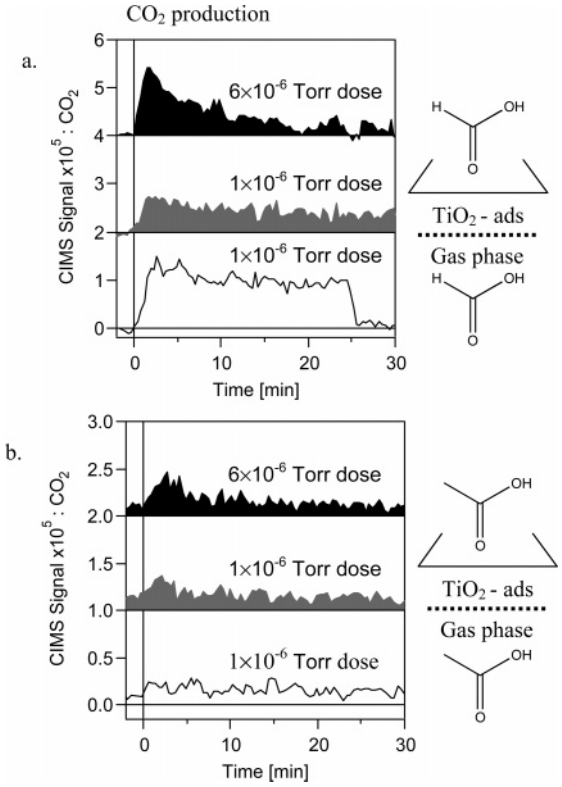

Figure 5. CO_2 production from (a) formic acid samples and (b) acetic acid samples. In both (a) and (b), the unfilled traces monitor gas phase photolysis near 1×10^{-6} Torr. The gray-filled traces and black-filled traces display CO_2 production following adsorption of $\sim 1 \times 10^{-6}$ and $\sim 6 \times 10^{-6}$ Torr carbonyl onto 10 layers of TiO_2, respectively. Traces have been offset vertically for clarity. In all cases the UV lights were turned on at 0 min.

Using formic and acetic acid, additional photochemistry experiments were performed in a manner analogous to the acetone experiments. Since formate has been suggested as an important acetone photocatalytic oxidation intermediate,[24,38,43,45,49,50,63] formic acid was used as a precursor for formate. The CO_2 production at 45 amu from this analyte is shown in Figure 5a. It is clear from Figure 5a that formate is efficiently converted into CO_2, both in the gas phase and after adsorption on TiO_2, and produces more CO_2 than was observed

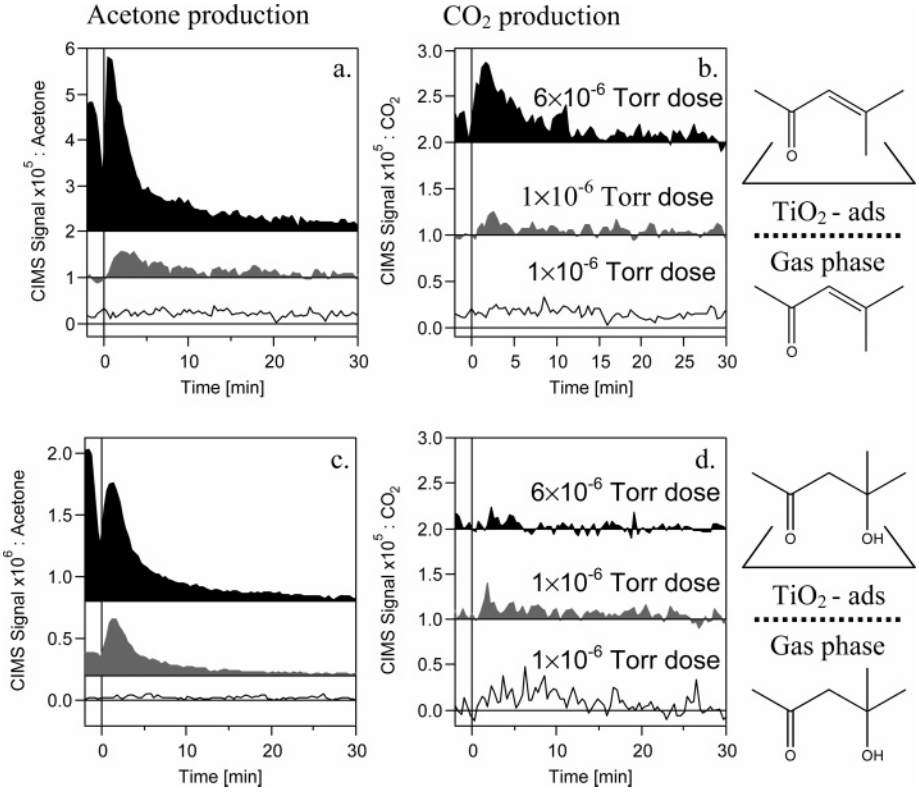

Figure 6. Photochemical production of (a) acetone and (b) CO_2 from mesityl oxide adsorbed onto TiO_2, and photochemical production of (c) acetone and (d) CO_2 from diacetone alcohol adsorbed onto TiO_2. In each panel, unfilled traces monitor gas phase photolysis near 1×10^{-6} Torr. The gray-filled traces and black-filled traces follow adsorption of $\sim 1 \times 10^{-6}$ and $\sim 6 \times 10^{-6}$ Torr carbonyl onto 10 layers of TiO_2, respectively. Traces have been offset vertically for clarity. In all cases the UV lights were turned on at 0 min.

using acetone as the test analyte. This may be due, in part, to the dissociative chemisorption interaction between formate and TiO_2.[70,71]

Similarly to formate, acetic acid is used as an acetate precursor on the TiO_2 catalyst.[69,71,76−80] Acetate is also thought to be a possible intermediate in the thermal decomposition[64] and photooxidation of acetone on TiO_2,[38,43,45,53] and similar reactivity between acetone and acetic acid analytes would provide support for this proposed mechanistic step. Our results indicate little gas phase photolysis at acetic acid partial pressures near 1×10^{-6} Torr (Figure 5b), and more production of CO_2 at both 1×10^{-6} and 6×10^{-6} Torr for acetic acid interacting with TiO_2 than is observed using acetone as the starting reactant. Acetic acid, however, produces less CO_2 than is observed using formic acid as a starting material. In the acetone and acid samples, no CIMS evidence for gas phase products other than CO_2 is observed.

b. Photooxidation of Mesityl Oxide and Diacetone Alcohol. After examination of acetone, and the proposed intermediates formed from acetic acid and formic acid adsorption, the acetone aldol products mesityl oxide and diacetone alcohol were studied in analogous experiments. In contrast to the results for acetone and the formic and acetic acids, the CIMS signal versus time traces exhibit production of gas phase species at the acetone mass signature. Figure 6a shows that when the mesityl oxide flow is reduced to zero, and the UV lights are turned on, the acetone CIMS signal increases rapidly. The same general behavior is seen in the CO_2 CIMS signal (Figure 6b). Acetone production occurs each time that adsorbed mesityl oxide is irradiated with UV light, while CO_2 production is less consistent between the two partial pressures examined. No significant production of acetone is observed in the control experiment performed without TiO_2 present. Together, these results indicate that acetone is an important photocatalytic product resulting from adsorbed mesityl oxide within the limits of our detection capabilities.

Similar behavior to that of mesityl oxide is seen for diacetone alcohol adsorbed on these Degussa P25 catalyst coatings (Figure 6c,d). Like the mesityl oxide samples, the CIMS signal versus time traces for diacetone alcohol photooxidation exhibit changes in the acetone CIMS signal intensity. As can be seen in Figure 6d, the acetone CIMS signal increases rapidly upon UV activation at both 1×10^{-6} and 6×10^{-6} Torr. In contrast to mesityl oxide, there is little evidence of the same increase in the CO_2 production. Without TiO_2 present, an increase in acetone is not detected in the gas phase (Figure 5c), but a small amount of CO_2 production is observed (Figure 6d). These observations indicate that acetone is also an important product resulting from UV irradiation of adsorbed diacetone alcohol within the limits of our detection.

c. Catalyst Activity. We quantify our observations regarding photooxidation by determining the peak areas in the CIMS versus time traces presented above. Our results yield a reasonable estimate for acetone production, in which we time-integrate the CIMS signal at 59 amu over 20 min following initiation of photolysis, and for CO_2 production, in which we integrate over both the mass peaks for CO_2 seen in Table 1. The integrated area is then divided by the time interval in seconds and the average surface coverage for that analyte partial pressure, as determined in section III1. A summary of the CO_2 and acetone production from the photochemistry experiments is shown in Figures 7a,b. Gas phase controls at analyte partial pressures near 1×10^{-6} Torr are included for comparison. For these controls, the area was found as in the experiments with TiO_2, but in this case the area is divided by the time interval and the number of molecules passing through the irradiated volume in that interval.

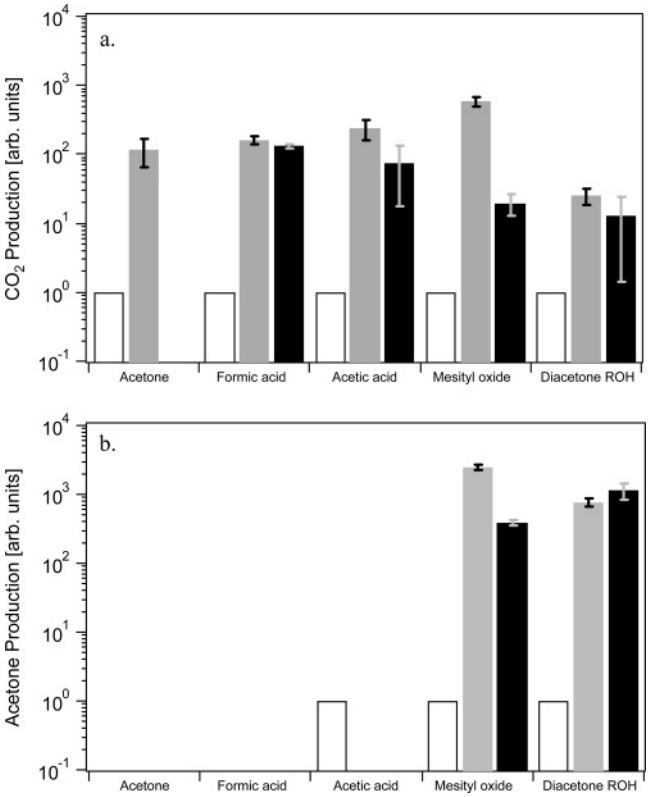

Figure 7. Peak areas from CIMS signal versus time traces for (a) CO_2 and (b) acetone production for each of the four analytes examined in this work, normalized to the results obtained for the gas phase experiments, in which no catalyst, but light, is present. Empty bars are results for 1×10^{-6} Torr in the gas phase, and gray-filled traces and black-filled bars result from the adsorption of 1×10^{-6} and 6×10^{-6} Torr carbonyl onto 10 layers of TiO_2, respectively. Error bars represent the variation between duplicate trials.

The latter value was calculated by estimating the gas velocity in the flow tube to be ~1000 cm s^{-1}.[65] Additionally, it should be noted that the adsorbed species in this work are exposed to ~6% of the photon flux incident on gas phase molecules due to UV absorption by the catalyst itself, and we therefore multiply the integrated areas by 0.06 to provide a meaningful lower estimate as a point of comparison for the heterogeneous process. After normalization to the gas phase CO_2 production, Figure 7a indicates that diacetone alcohol is the species least efficiently converted into CO_2. Mesityl oxide produces more CO_2 when 1×10^{-6} Torr is adsorbed on the catalyst than at the higher partial pressure. Aside from mesityl oxide, formic acid is the species most efficiently and consistently converted from a surface species to gas phase CO_2. The next most effectively converted species is acetate formed following acetic acid adsorption. Although adsorbed diacetone alcohol and mesityl oxide produce some CO_2, it is clear that both species are also likely to produce acetone.

d. Catalyst Poisoning. The inefficient conversion of adsorbates to CO_2 and H_2O may result in surface species that deactivate the catalyst toward further adsorption and/or heterogeneous photocatalytic oxidation. It has been postulated that condensation products, in particular, may act as surface poisons during the adsorption and subsequent photocatalytic oxidation of ketones on metal oxides if the condensation process is strongly favored.[51,54] Additionally, if condensation products react more slowly or less efficiently than acetone, as has been reported,[24,39] they should decrease the overall acetone photocatalytic oxidation rate. To determine the likelihood of condensation species accumulating at low partial pressures on

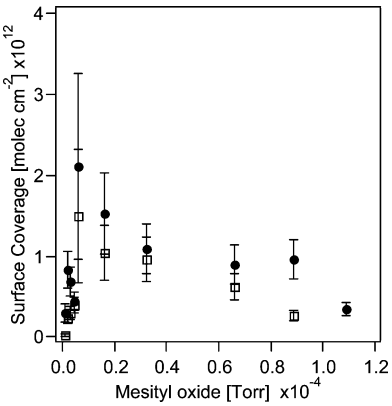

Figure 8. Adsorption isotherm for mesityl oxide on Degussa P25 TiO_2 measured between 9×10^{-7} and 1.1×10^{-6} Torr. Closed circles represent the net adsorption of molecules from the gas phase onto the catalyst surface, and open squares represent the return of molecules to the gas phase following adsorption, i.e., reversible adsorption onto the catalyst coating.

powdered substrates such as the coatings used in this work, we measure an adsorption isotherm for mesityl oxide on 10 layers of TiO_2 in the manner reported previously for measuring acetone adsorption isotherms.[65,66] The isotherms for both the net adsorption and reversible adsorption (i.e., the desorbing molecules) are shown in Figure 8. The adsorption of mesityl oxide decreases slightly as the catalyst coating is sequentially exposed to increasing mesityl oxide partial pressures between $\sim 1 \times 10^{-6}$ and 1×10^{-4} Torr. This suggests that mesityl oxide adsorption may saturate the TiO_2 surface in the absence of UV light. This result supports the idea that acetone condensation products may act as catalyst poisons. Figure 7b, however, suggests that UV irradiation of acetone condensation products adsorbed on TiO_2 return acetone to the gas phase. This finding is in agreement with the observation by Giffiths et al., who reported that some acetone is formed from the degradation of mesityl oxide.[59] These results imply that under *operando* conditions, that is, under working catalyst conditions of low temperature, low acetone partial pressures, and with the use of UV lighting, condensation products on Degussa P25 are not likely to poison the catalyst. If condensation products do accumulate on the TiO_2 surface during acetone adsorption in the dark, subsequent UV irradiation will either transform a large portion of the surface mesityl oxide and/or diacetone alcohol to acetone or oxidize some of the condensation product directly in the case of mesityl oxide. The efficiency of this transformation under *operando* conditions will determine whether catalytic sites are poisoned by the high molecular weight condensation products and others are regenerated though partial or full oxidation chemistry.

IV. Physical Interpretation and Environmental Implications

The efficient removal of VOCs such as acetone from indoor environments has focused on heterogeneous photocatalysis over titanium dioxide because of the ability of this oxide to accelerate the degradation of adsorbed organic compounds[13,17,23−25] compared to the gas phase. The data in Figure 7 clearly indicate that on a per molecule and per UV photon basis, the heterogeneous process is 1−2 orders of magnitude more efficient than gas phase photolysis in mineralizing the VOCs examined in this work. The photooxidation studies reported here indicate efficient conversion of carboxylate species, particularly formate, to CO_2 under our experimental conditions. This is not surprising given the thermodynamic stability of CO_2 versus formic acid.

Nor is it surprising that formic acid is more easily mineralized than higher molecular weight species in which the transition state presumably looks less like the final CO_2 product. Furthermore, acetone aldol condensation may not result in catalyst poisoning, because we find that mesityl oxide and diacetone alcohol decompose to form gas phase acetone when the TiO_2 surface is exposed to UV light. However, this reaction does little to abate acetone pollution in the indoor environment because acetone is regenerated from these species. Additionally, if the catalyst is kept in dark conditions for prolonged periods, where condensation reactions can saturate the surface, these products may prevent further acetone adsorption.

Several proposed mechanisms support the observations reported here, suggesting that carboxylate species, and in particular formate,[24,38,43,49,50,63] are important intermediates during acetone oxidation. Coronado et al.[43] observed the formation of both surface acetate and formate as primary pathways for acetone photooxidation on anatase TiO_2 near room temperature. Xu et al.[49,50] have suggested an alternative mechanism in which acetone undergoes aldol condensation to form mesityl oxide, which then reacts with molecular oxygen to form surface-bound formate. The formate species then reacts to produce CO_2. Henderson's UHV work with acetone interacting with rutile (110) single crystals at 105 K suggests that methyl radicals may form surface formate in higher pressure experiments on powdered catalyst samples.[53] Clearly, there are several reaction pathways that could produce reactive formate species, underscoring the importance of this species as an intermediate in the overall photooxidation of acetone.

Our work suggests that mechanisms that proceed through surface formate or acetate are likely to be the most effective at mineralizing acetone at environmentally relevant partial pressures and temperatures. The greatest difference between our results and work by others is that we find that acetone does not degrade readily on Degussa P25 under environmentally representative partial pressures and low-intensity UV irradiation. This implies that catalysts that can transform acetone to surface formate are highly desirable.

Since carboxylate species are expected to be more efficiently mineralized than aldol condensation products, surface condensation reactions should be minimized in catalytic systems for indoor applications. Mesityl oxide formation on metal oxides is favored at high acetone surface coverages,[6] elevated temperature,[48,54] and low relative humidity,[24] so efficient indoor acetone mineralization should avoid these conditions. Additionally, mesityl oxide is associated with surface Lewis acid sites rather than surface hydroxyl species,[59] so high hydroxyl surface densities or low surface acid site densities may prevent acetone condensation.

Tailoring titanium dioxide catalyst surfaces for specific applications has a long tradition[12,17,26,70] with too many studies to review here. However, it should be noted that TiO_2 doped with carbon,[81] nitrogen,[82] or niobium[83] have recently been applied to the degradation of acetone. This work suggests that modifying TiO_2-based catalysts to promote the formation of carboxylate intermediates as opposed to condensation products is desirable. Under conditions representative of those found indoors, where acetone partial pressures and temperature are low, condensation processes may not be favored, and catalysts that enhance formate production from acetone precursors are likely to provide the best environmental remediation of acetone. A focus on the acetone to formate transformation therefore represents a worthwhile area of catalyst development.

V. Summary

On the basis of an analysis of the relative production of carbon dioxide, we have determined the photooxidation activities of several possible intermediates in the mechanism for acetone photooxidation on Degussa P25 TiO_2 powders. We also report uptake coefficients for each species. Uptake coefficients and competition experiments between acetone and acetic acid indicate that acetic acid, and by extension formic acid, is tightly bound to the surface, where it can inhibit acetone binding to the surface. The lower uptake coefficients for acetic acid and formic acid compared to higher molecular weight species suggest dissociative adsorption of the former species, which results in surface acetate and formate species. The carboxylate species consistently produce only CO_2 after exposure of Degussa P25 to low reactant partial pressures and UV irradiation. In contrast, although aldol products such as mesityl oxide and diacetone alcohol produce CO_2, they also return acetone to the gas phase under these conditions. The data presented here imply that mechanisms that emphasize aldol condensations as reactive pathways to produce CO_2, though active and important for conditions of high acetone partial pressure, high temperature, and/or low relative humidity, may not be important under environmental conditions. In realistic indoor environments, acetone is present at low partial pressures such as the ones employed in this work, and low- or room-temperature photocatalysis would be preferred to reduce the energy cost of remediation processes. In such environments, catalyst surfaces that enhance formate and acetate production from acetone are likely to provide efficient acetone remediation in indoor environments.

Acknowledgment. We gratefully acknowledge the kind donation of Degussa P25 to Professor Kimberly Gray at Northwestern University by the Degussa Corp. We also thank Aditya Savara for providing FTIR spectra, Dr. Julianne Gibb-Davis and Patrick Hayes for collecting NMR data, and Jeremy Barton for providing SEM images. We acknowledge support of this research by the Chemical Sciences, Geosciences and Biosciences Division, Office of Basic Energy Sciences, Office of Science, U.S. Department of Energy (Grant No. DE-FG02-03ER15457), the National Science Foundation Division of Atmospheric Sciences (Grant No. ATM-0533634), the American Chemical Society Petroleum Research Fund (Grant No. 38960-G5S), and a Dow Chemical Co. professorship to FMG. FMG is a Sloan Fellow (2007-2009).

Supporting Information Available: Textual explanation of UV−vis transmission of catalyst coatings, analyte characterization, and CIMS peak identification. Tables of fitting parameters, NMR data, and uptake coefficients. Figures of FTIR and CIMS spectra. This material is available free of charge via the Internet at http://pubs.acs.org.

References and Notes

(1) Finlayson-Pitts, B. J.; Pitts, J. N. *Chemistry of the Upper and Lower Atmosphere: Theory, Experiments, and Applications*; Academic Press: New York, 2000.

(2) Jenkins, P. L.; Phillips, T. J.; Mulberg, E. J.; Hui, S. P. *Atmos. Environ. A-Gen.* **1992**, *26*, 2141.

(3) "The Inside Story: A Guide to Indoor Air Quality," United States Environmental Protection Agency and the United States Consumer Product Safety Commission Office of Radiation and Indoor Air (6604J), 1995.

(4) Shah, J. J.; Singh, H. B. *Environ. Sci. Technol.* **1988**, *22*, 1381.

(5) Spengler, J. D.; Chen, Q. Y. *Annu. Rev. Energ. Environ.* **2000**, *25*, 567.

(6) American Society of Heating, Refrigerating and Air-Conditioning Engineers (ASHRAE). Position Papers: Indoor Air Quality, 2001.

(7) EPA-402-S-01-001 "Energy cost and IAQ: Performance of ventilation systems and controls. (a) Project Report #4. Impacts of increased outdoor air flow rates on annual HVAC energy costs. (b) Project Report #5. Peak load impacts of increasing outdoor air flows from 5 cfm to 20 cfm per occupant in large office buildings", United States Environmental Protection Agency, Indoor Environments Division (6609J), Office of Air and Radiation, 2000.

(8) Fanger, P. O. *Indoor Air* **2006**, *16*, 328.

(9) Fisk, W. J.; Rosenfeld, A. H. *Indoor Air-Int. J. Indoor Air Qual. Clim.* **1997**, *7*, 158.

(10) Fisk, W. J.; Brager, G.; Brook, M.; Burge, H.; Cole, J.; Cummings, J.; Levin, H.; Loftness, V.; Logee, T.; Mendell, M. J.; Persily, A.; Taylor, S.; Zhang, J. F. "A priority agenda for energy-related indoor environmental quality research"; Proceedings: Indoor Air, 2002, Monterey, CA.

(11) Mendell, M. J.; Fisk, W. J.; Kreiss, K.; Levin, H.; Alexander, D.; Cain, W. S.; Girman, J. R.; Hines, C. J.; Jensen, P. A.; Milton, D. K.; Rexroat, L. P.; Wallingford, K. M. *Am. J. Public Health* **2002**, *92*, 1430.

(12) Fox, M. A.; Dulay, M. T. *Chem. Rev.* **1993**, *93*, 341.

(13) Hodgson, A. T.; Destaillats, H.; Sullivan, D. P.; Fisk, W. J. *Indoor Air* **2007**, ASAP.

(14) Herrmann, J. M. *Catal. Today* **1995**, *24*, 157.

(15) Hoffmann, M. R.; Martin, S. T.; Choi, W. Y.; Bahnemann, D. W. *Chem. Rev.* **1995**, *95*, 69.

(16) Kamat, P. V. *Chem. Rev.* **1993**, *93*, 267.

(17) Linsebigler, A. L.; Lu, G. Q.; Yates, J. T. *Chem. Rev.* **1995**, *95*, 735.

(18) Larson, S. A.; Widegren, J. A.; Falconer, J. L. *J. Catal.* **1995**, *157*, 611.

(19) Fujishima, A. R.; Tata, N.; Tryk Donald, A. *J. Photochem. Photobiol. C* **2000**, *1*, 1.

(20) Miller, R.; Fox, R. Treatment of organic contaminants in air by photocatalytic oxidation: A commercialization perspective. In *Photocatalytic Purification and Treatment of Water and Air*; Ollis, D. F., Al-Ekabi, H., Eds.; Elsevier: Amsterdam, 1993; Vol. 3, pp 573.

(21) Wang, K.-M.; Marinas, B. J. Control of VOC emissions from air-stripping towers: Development of gas-phase photocatalytic process. In *Photocatalytic Purification and Treatment of Water and Air*; Ollis, D. F., Al-Ekabi, H., Eds.; Elsevier: Amsterdam, 1993; Vol. 3, pp 733.

(22) Frazer, L. *Environ. Health Perspect.* **2001**, *109*, A174.

(23) Alberici, R. M.; Jardim, W. E. *Appl. Catal. B-Environ.* **1997**, *14*, 55.

(24) El-Maazawi, M.; Finken, A. N.; Nair, A. B.; Grassian, V. H. *J. Catal.* **2000**, *191*, 138.

(25) Vorontsov, A. V.; Savinov, E. N.; Barannik, G. B.; Troitsky, V. N.; Parmon, V. N. *Catal. Today* **1997**, *39*, 207.

(26) Thompson, T. L.; Yates, J. T. *Chem. Rev.* **2006**, *106*, 4428.

(27) Gerischer, H. Conditions for an efficient photocatalytic activity of TiO_2 particles. In *Photocatalytic Purification and Treatment of Water and Air*; Ollis, D. F., Al-Ekabi, H., Eds.; Elsevier: Amsterdam, 1993; Vol. 3, pp 1.

(28) Finlayson-Pitts, B. J.; Pitts, J. N., Jr. *Chemistry of the Upper and Lower Atmosphere*; Academic Press: New York, 2000.

(29) Peral, J.; Ollis, D. F. *J. Catal.* **1992**, *136*, 554.

(30) Daisey, J. M.; Hodgson, A. T.; Fisk, W. J.; Mendell, M. J.; Tenbrinke, J. *Atmos. Environ.* **1994**, *28*, 3557.

(31) Baez, A.; Padilla, H.; Garcia, R.; Torres, M. D.; Rosas, I.; Belmont, R. *Sci. Total Environ.* **2003**, *302*, 211.

(32) Ten Brinke, J.; Selvin, S.; Hodgson, A. T.; Fisk, W. J.; Mendell, M. J.; Koshland, C. P.; Daisey, J. M. *Indoor Air-Int. J. Indoor Air Qual. Clim.* **1998**, *8*, 140.

(33) Wolkoff, P.; Nielsen, G. D. *Atmos. Environ.* **2001**, *35*, 4407.

(34) Brown, S. K.; Sim, M. R.; Abramson, M. J.; Gray, C. N. *Indoor Air-Int. J. Indoor Air Qual. Clim.* **1994**, *4*, 123.

(35) Lagoudi, A.; Loizidou, M.; Asimakopoulos, D. *Indoor Built Environ.* **1996**, *5*, 348.

(36) Feng, Y.; Wen, S.; Wang, X.; Sheng, G.; He, Q.; Tang, J.; Fu, J. *Atmos. Environ.* **2004**, *38*, 103.

(37) Jurvelin, J. A.; Edwards, R. D.; Vartiainen, M.; Pasanen, P.; Jantunen, M. J. *J. Air Waste Manage. Assoc.* **2003**, *53*, 560.

(38) Zhu, X. Synthesis of oxynitrides and nitrogen-doped titania and FTIR studies of thermal and photooxidation of acetone on titania. Ph.D. (Doctoral) Thesis, Northwestern University, 2006.

(39) Choi, W.; Ko, J. Y.; Park, H.; Chung, J. S. *Appl. Catal. B-Environ.* **2001**, *31*, 209.

(40) Zorn, M. E.; Tompkins, D. T.; Zeltner, W. A.; Anderson, M. A. *Appl. Catal. B-Environ.* **1999**, *23*, 1.

(41) Vorontsov, A. V.; Kurkin, E. N.; Savinov, E. N. *J. Catal.* **1999**, *186*, 318.

(42) Vorontsov, A. V.; Stoyanova, I. V.; Kozlov, D. V.; Simagina, V. I.; Savinov, E. N. *J. Catal.* **2000**, *189*, 360.

(43) Coronado, J. M.; Kataoka, S.; Tejedor-Tejedor, I.; Anderson, M. A. *J. Catal.* **2003**, *219*, 219.

(44) Coronado, J. M.; Zorn, M. E.; Tejedor-Tejedor, I.; Anderson, M. A. *Appl. Catal. B-Environ.* **2003**, *43*, 329.

(45) Yats'kiv, V. I.; Granchak, V. M.; Kovalenko, A. S.; Tsyrina, V. V.; Il'in, V. G.; Kuchmii, S. Y. *Theor. Exp. Chem.* **2003**, *39*, 48.

(46) Ibrahim, H.; de Lasa, H. I. *AIChE J.* **2004**, *50*, 1017.

(47) Li, P.; Perreau, K. A.; Covington, E.; Song, C. H.; Carmichael, G. R.; Grassian, V. H. *J. Geophys. Res.-Atmos.* **2001**, *106*, 5517.

(48) Zaki, M. I.; Hasan, M. A.; Pasupulety, L. *Langmuir* **2001**, *17*, 768.

(49) Xu, W. Z.; Raftery, D. *J. Catal.* **2001**, *204*, 110.

(50) Xu, W. Z.; Raftery, D.; Francisco, J. S. *J. Phys. Chem. B* **2003**, *107*, 4537.

(51) Luo, S. C.; Falconer, J. L. *J. Catal.* **1999**, *185*, 393.

(52) Attwood, A. L.; Edwards, J. L.; Rowlands, C. C.; Murphy, D. M. *J. Phys. Chem. A* **2003**, *107*, 1779.

(53) Henderson, M. A. *J. Phys. Chem. B* **2005**, *109*, 12062.

(54) Zaki, M. I.; Hasan, M. A.; Al-Sagheer, F. A.; Pasupulety, L. *Langmuir* **2000**, *16*, 430.

(55) Masel, R. I. *Principles of Adsorption and Reactions on Solid Surfaces*; John Wiley & Sons: New York, 1996.

(56) Somorjai, G. A. *Introduction to Surface Chemistry and Catalysis*; John Wiley & Sons: New York, 1994.

(57) Biaglow, A. I.; Sepa, J.; Gorte, R. J.; White, D. *J. Catal.* **1995**, *151*, 373.

(58) Fouad, N. E.; Thomasson, P.; Knozinger, H. *Appl. Catal. A-Gen.* **2000**, *196*, 125.

(59) Griffiths, D. M.; Rochester, C. H. *J. Chem. Soc.-Faraday Trans.* **1978**, *74*, 403.

(60) Kubelkova, L.; Cejka, J.; Novakoya, J. *Zeolites* **1991**, *11*, 48.

(61) Kubelkova, L.; Novakova, J. *Zeolites* **1991**, *11*, 822.

(62) Panov, A. G.; Fripiat, J. J. *J. Catal.* **1998**, *178*, 188.

(63) Hagglund, C.; Kasemo, B.; Osterlund, L. *J. Phys. Chem. B* **2005**, *109*, 10886.

(64) Henderson, M. A. *J. Phys. Chem. B* **2004**, *108*, 18932.

(65) Schmidt, C. M.; Weitz, E.; Geiger, F. M. *Langmuir* **2006**, *22*, 9642.

(66) Schmidt, C. M.; Savara, A.; Weitz, E.; Geiger, F. M. *J. Phys. Chem. C* **2007**, *111*, 8260.

(67) Herbert, C. G.; Johnstone, R. A. W. *Mass Spectrometry Basics*; CRC Press LLC: Boca Raton, FL, 2002.

(68) Atkins, P. *Physical Chemistry*, 6th ed.; W.H. Freeman and Co.: New York, 1998.

(69) Kim, K. S.; Barteau, M. A. *Langmuir* **1988**, *4*, 945.

(70) Diebold, U. *Surf. Sci. Rep.* **2003**, *48*, 53.

(71) Tanner, R. E.; Liang, Y.; Altman, E. I. *Surf. Sci.* **2002**, *506*, 251.

(72) Altman, E. I.; Tanner, R. E. *Catal. Today* **2003**, *85*, 101.

(73) Adamson, A. W.; Gast, A. P. *Physical Chemistry of Surfaces*, 6th ed.; John Wiley & Sons: New York, 1997.

(74) N.I.S.T. Proton Affinity Database; NIST (National Institute of Standards and Technology), 2005.

(75) Lindinger, W.; Hansel, A. *Plasma Sources Sci. Technol.* **1997**, *6*, 111.

(76) Guo, Q.; Cocks, I.; Williams, E. M. *J. Chem. Phys.* **1997**, *106*, 2924.

(77) Muggli, D. S.; Falconer, J. L. *J. Catal.* **1999**, *187*, 230.

(78) Liao, L. F.; Lien, C. F.; Lin, J. L. *Phys. Chem. Chem. Phys.* **2001**, *3*, 3831.

(79) Idriss, H.; Legare, P.; Maire, G. *Surf. Sci.* **2002**, *515*, 413.

(80) Rachmady, W.; Vannice, M. A. *J. Catal.* **2002**, *207*, 317.

(81) Irie, H.; Watanabe, Y.; Hashimoto, K. *Chem. Lett.* **2003**, *32*, 772.

(82) Ihara, T.; Miyoshi, M.; Iriyama, Y.; Matsumoto, O.; Sugihara, S. *Appl. Catal. B-Environ.* **2003**, *42*, 403.

(83) Mattsson, A.; Leideborg, M.; Larsson, K.; Westin, G.; Osterlund, L. *J. Phys. Chem. B* **2006**, *110*, 1210.